Chemical Methodologies 6(2022) 977-984

Chemical Methodologies

Journal homepage: http://chemmethod.com

Original Research Article

Spectroscopic Study of Iron Oxide Nanoparticles Synthesized *Via* Hydrothermal Method

Ahmed B. Taha[1,2]*, Mohammed Sh. Essa[3], Bahaa T. Chiad[1]

[1]*Department of Physics, College of Science, University of Baghdad, Baghdad, Iraq*
[2]*Department of Optics Techniques, College of Health and Medical Technology, University of Uruk, Iraq*
[3]*Department of Medical Physics, College of Applied Science, University of Fallujah, Iraq*

ARTICLE INFO

Article history

Submitted: 2022-06-07
Revised: 2022-07-09
Accepted: 2022-09-12
Manuscript ID: CHEMM-2208-1590
Checked for Plagiarism: Yes
Language Editor:
Dr. Fatimah Ramezani
Editor who approved publication:
Dr. Mohsen Oftadeh

DOI:10.22034/CHEMM.2022.355199.1590

KEYWORDS

Hydrothermal
Iron Oxide
XRD

ABSTRACT

Iron oxide nanoparticles are one of the most important materials in nanotechnology due to their unique properties in many fields. In this research, iron oxide nanoparticles are synthesized by using new homemade autoclave reactor with hydrothermal method. Many studies of iron oxide nanoparticles have been studies, including surface morphology, structural morphology, and optical studies. The XRD characteristics of the pattern show very thin peaks, indicating the nanoparticles formation with average crystallite size about 26 nm. The SEM and FE-SEM analyses reveal the formation of the nanoparticles with spherical shape and size ranging from 35 nm to 45 nm. The spherical particles are exhibiting the high levels of aggregation due to the innate tendency to the magnetic characteristics. The EDX verified that there were only percentages of oxygen and iron in the nanoparticles. The FT-IR analysis for the iron oxide showed that the absorption peaks at about 430 and 630 cm^{-1} are observed corresponding to stretching modes of the Fe-O bond in maghemite. Finally, the optical properties of the iron oxide sample reveal a broad absorption band area with energy band gap about (2.08 eV) which are nearly about the energy band gap of standard iron oxide which is equal to (2.2 eV). Therefore, all studies showed the autoclave reactor is a powerful tool to form iron oxide nanoparticles with a high purity and the ultra-fine particle size.

GRAPHICAL ABSTRACT

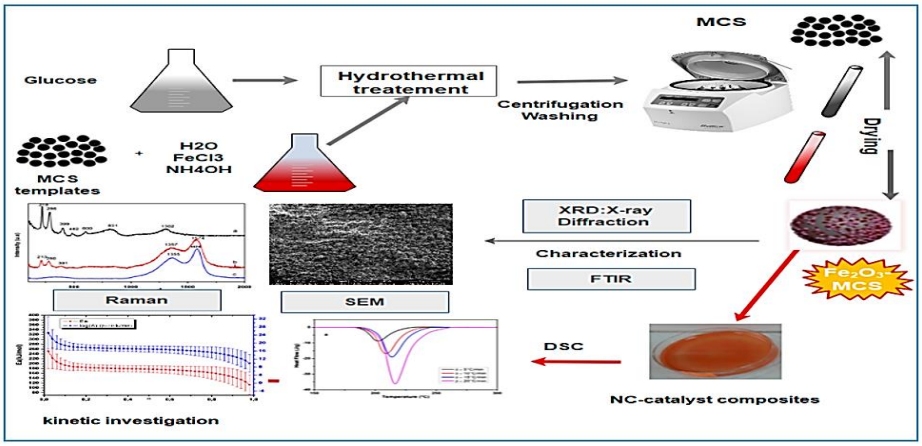

* Corresponding author: Ahmed B. Taha
✉ E-mail: ahmeddbasim0@gmail.com

Introduction

Recently, nanotechnology has become one of the most interesting fields' frontier disciplines in science and technology. Different synthesis approaches have found a wide range of applications for various types of nanoparticles with different features [1]. Because of their unique magnetic, optical, and electrical capabilities, iron oxide nanoparticles have attracted a lot of attention [2]. Magnetic nanoparticles have been synthesized by using the hydrothermal process, co-precipitation, micro emulsion, thermal decomposition, sol-gel processing, and other methods [3-7]. One such nanoparticle is the magnetic nanoparticle that is of high significance for the scientists around the world, which is being used in magnetic ink [8], magnetic storage tape and devices [9], medicine and medical diagnosis, MRI as a contrast agent [10], gene and drug delivery, and cancer hyperthermia [11].

Iron oxide have many advantages, such as narrow band gap energy of approximately 2.2 eV, low cost, non-toxicity, availability, and thermal stability. Magnetite contains iron types, namely ferrous and ferric. Thus, it is usually described as iron II and III oxide. In nature, there are three main types of iron oxides: maghemite (γ-Fe_2O_3), magnetite (Fe_3O_4), and hematite (α-Fe_2O_3) [12].

Hematite's (α-Fe_2O_3) unit cell is hexagonal and only contains octahedral coordinated Fe^{+3} atoms (corundum structure), while γ-Fe_2O_3 (magnetite) particles have the cubic unit cells with both octahedral and tetrahedral coordinated Fe^{+3} sites (the defect spinel structure) [13].

Any heterogeneous reaction taking place in the presence of aqueous solvents or mineralizers under the high pressures and temperatures to dissolve and recrystallize materials that are insoluble under ordinary circumstances is known as hydrothermal processing [14]. Furthermore, the technique makes possible the energy savings, better nucleation control, pollution avoidance, higher dispersion, higher reaction rates, better shape control, and lower temperature operations in the solvent presence [15]. In this study, the iron oxide nanoparticles were prepared by Hydrothermal method and their characterization was studied.

Materials and Methods

The preparation process is done by using an aqueous solution of ferric chloride anhydrous $FeCl_3$ dissolved in distilled water, and then preparing of ferrous sulphate ($FeSO_4.7H_2O$) dissolved in distilled water with 1:2 molarity ratio. The solutions of the two salts were mixed. Then, ammonium hydroxide NH_4OH was added to the mixture continuously until the pH changed to 11–13, after that the NH_4OH addition was stopped when black precipitate is formed on the mixture with stirring for 10 minutes. the mixture of the black precipitate inserted in homemade (Teflon lined stainless autoclave) inside the oven at 150 °C for 2 hours, as displayed in Figure 1 for the system plotted by 3D max and Photoshop programs for the designed autoclave. After the reaction was finished, the autoclave was cooled at room temperature and the solution was separated from particles by magnet, and then centrifuged for 20 minutes with 1000 rpm. After that, it was washed with ethanol and distilled water for 3 times. Next, the sample dried at 45 °C in oven for 24 hours to produce the black powder of iron oxide.

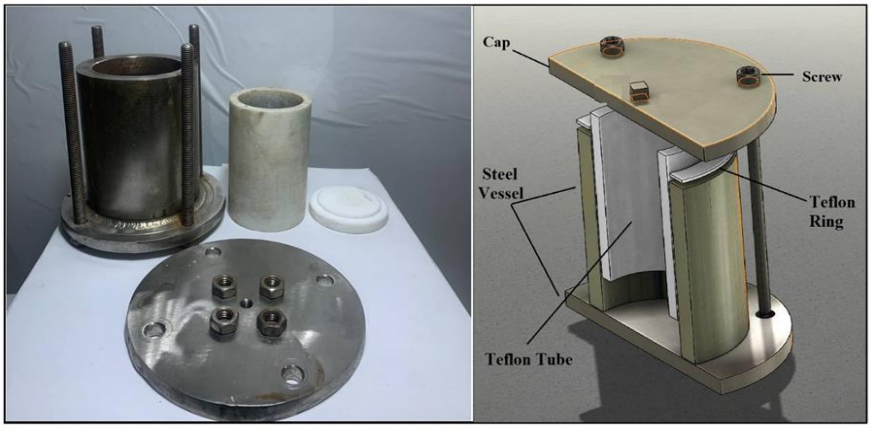

Figure 1: Home-made teflon lined stainless autoclave

Results and Discussion

The XRD pattern of iron oxide prepared by the hydrothermal method is depicted in Figure 2. The XRD pattern shows very thin peaks, indicating the nanoparticles formation with an average size varied from 15 to 39 nm. This small size indicates that the preparation of iron oxide by this autoclave specification give very small size nanoparticles that could be used in many applications.

It was noted that the products revealed a cubic spinal structure with a good crystallinity that had a characteristic peak matching with the standard structure of maghemite (JCPDS 39-1346) [16]. The peaks were visible at 2θ≈ 30.45° (220), 35.67° (311), 43.35 (400), 53.9° (422), 57.4° (511) and 62.93° (440) for iron oxide, no other impurity peaks for other materials or iron phase are seen, indicating that the prepared nanoparticles are pure iron oxide.

The prepared nanoparticles by this method are well crystallized, as seen by the strong peaks in XRD patterns, while the peak broadening clearly demonstrates the nanocrystals formation of small size in the sample. Therefore, to calculate the particle size, the peak broadening at a smaller angle is more significant. Thus, the particle size of nanoparticles was calculated by using a high intensity peak (311) at 2θ value 35.67° for γ-Fe_2O_3 nanoparticles. The calculated particle size is found to be 15.18 nm. The crystallite size was obtained by using Bragg formula and the calculated cell parameter according to Scherer's equation, as illustrated in Table 1.

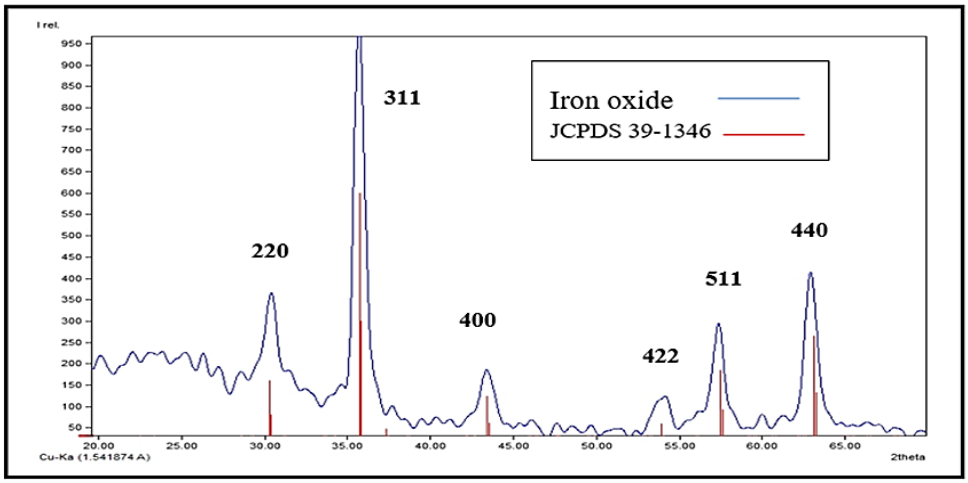

Figure 2: X-ray diffraction of iron oxide nanoparticles

Table 1: The crystallite size and the cell parameter of iron oxide nanoparticles synthesized by the Hydrothermal method

D(nm)	d(A^0)	h	k	l	a(A^0)
39.72	2.93	2	2	0	8.30
15.19	2.52	3	1	1	8.34
28.49	2.09	4	0	0	8.34
29.72	1.70	4	2	2	8.31
20.19	1.60	5	1	1	8.33
31.08	1.48	4	4	0	8.35

The surface morphology of synthesis iron oxide was investigated by using SEM and FESEM. We have studied the surface morphology properties of the iron oxide prepared by hydrothermal method. SEM confirmed the spherical morphology and narrow size distribution with nano structure of the iron oxide nanoparticles, as depicted in Figure 3.

The surface morphology of the prepared iron oxide particles is studied by FESEM, as demonstrated in Figure 4. The FESEM micrographs of iron oxide nanoparticles are

showed the particles formation with spherical shaped. Nano sized whose size is varying from 35 nm to 45 nm with high levels of aggregation is due to the natural tendency of the iron oxide nanoparticles to aggregate as a result of their magnetic characteristics. In addition, there is a significant particle aggregation due to the uncapped, very small size of the produced iron oxide nanoparticles which confirmed the nanoparticles formation.

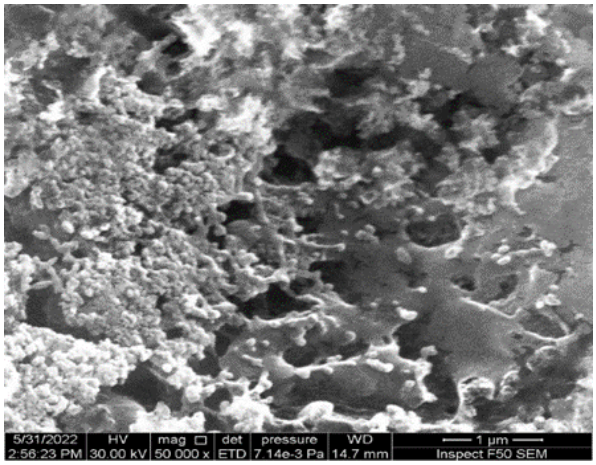

Figure 3: The electron microscopy scanning of prepared iron oxide by hydrothermal method

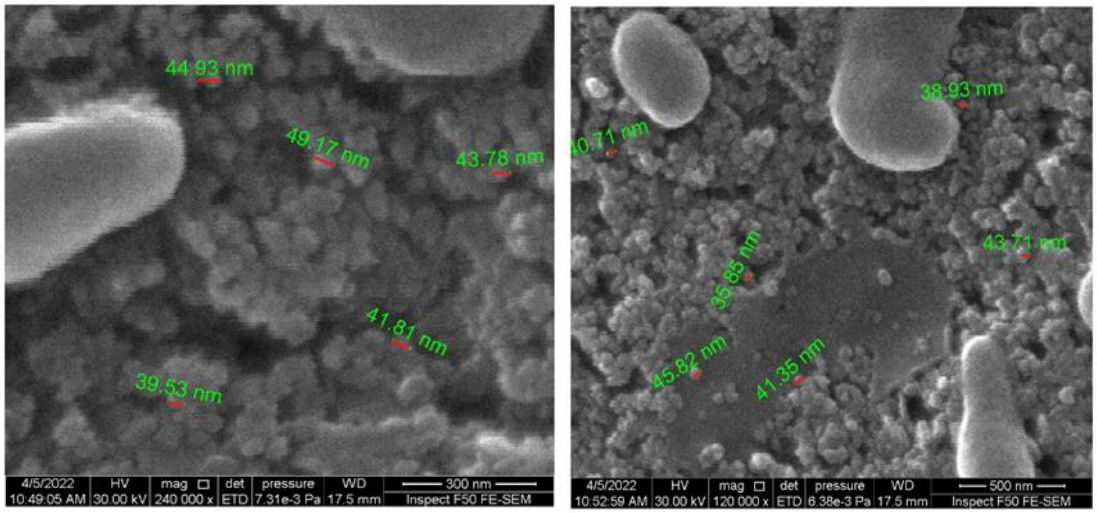

Figure 4: The field-emission scanning electron microscopy of prepared iron oxide nanoparticles (a) FESEM with 300 nm length scale and (b) FESEM with 500 nm length scale

The synthesized iron oxide nanoparticles purity was studied by using the Energy Dispersive X-ray spectroscopy (EDX) The EDX spectra in Figure 5 showed only peaks of oxygen and iron, the peaks around 6.41 keV are associated to the binding energies of iron, while the peak of oxygen at 0.42 keV. Consequently, the EDX verified that there was oxygen and iron in the nanoparticles. The Fe normal weight was (73.18 %), while the normal weight of O was (26.82%).

The additional investigation has been done on the structural characteristics of the nanoparticles, The FT-IR analysis measurements are depicted in Figure 6. The absorption peak at about 563 cm^{-1} and 631 cm^{-1} are correspond to stretching modes of the maghemite (Fe-O), the absorption peaks of the OH functional group (3800–3600 cm^{-1}), some peaks corresponding to other organic compounds were observed and presented in Table 2. These absorption peaks are in agreement with the literature values [17-21].

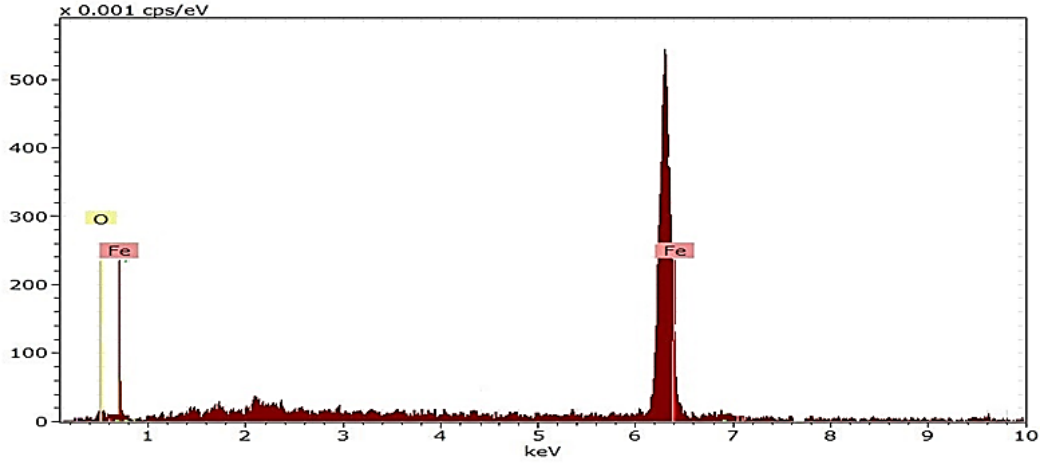

Figure 5: Energy dispersive X-ray spectrum of iron oxide nanoparticles

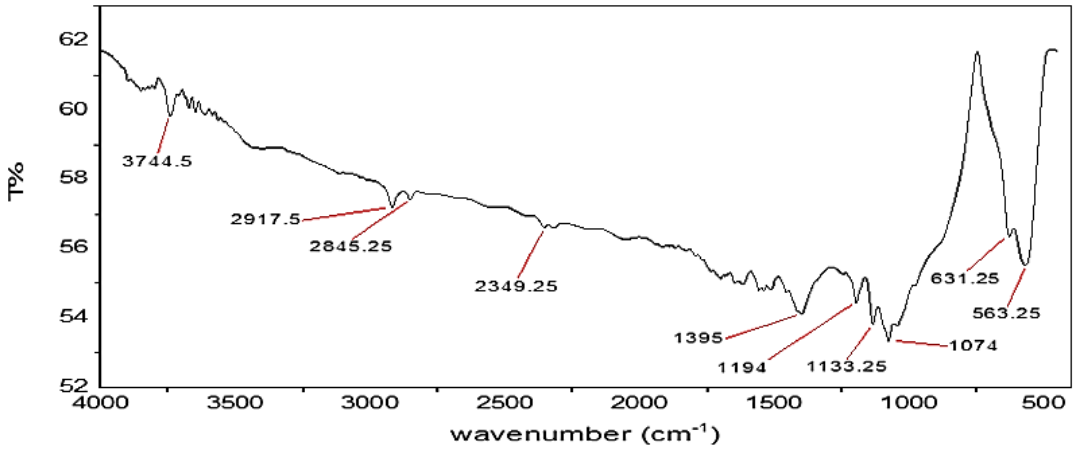

Figure 6: The FT-IR spectrum of iron oxide nanoparticles synthesized by the Hydrothermal method

Table 2: The FT-IR Frequency range and functional groups of iron oxide nanoparticles

Frequency range	Functional groups	Vibration
3745.5	OH Amid	Stretching
2917.5	C-H	Stretching a symmetric
2845.25	C-H_2	Stretching symmetric
1395	O-H	Bending
1194	-C-O	Stretching
1133.25	C–O–C	Stretching
1074	C-O	Stretching
631.25	Fe-O	Stretching
563.25	Fe-O	Stretching

The optical properties of the iron oxide sample were determined through UV-VIS by (k-mac spectra academy sv-2100); the following UV-visible light spectroscopy results were measured in the wavelength ranging from 400 nm to 800 nm. The optical absorbance spectra of the iron oxide sample are demonstrated in Figure 7. The absorption spectra of the iron oxide nanoparticles illustrate a broad absorption band area. This broadening may be attributed to the adsorbed molecules that also appear in SEM and FE-SEM.

The absorption curve reveals the iron oxide nanoparticles that reach the maximum absorption edge from 500 to 530 nm with three peaks due to different vibrational and rotational transitions from ground state to an excited state associated

with the electronic transition. The higher energy peaks are due to transitions to higher electronic excited state. Therefore, each of this associated transition has a slightly different absorption value. Tuac's equations were used to calculate the optical band gap: $(\alpha h\nu)^n = A (h\nu - Eg)$, where (hv) is the energy of photon, (A) is the constant related to the material, and n is 2 for the direct transition and 1/2 for the indirect transition. As a result, by projecting the linear component of the $(\alpha h\nu)^n - h\nu$ curve to zero, the optical band gap for the absorption peak can be obtained, as depicted in the Figure 8. Therefore, the calculated optical band gap for iron oxide nanoparticles was found about (2.08 eV). This value was nearly to the band gap of standard iron oxide which is equal to (2.2 eV) with a small difference due to the aggregation of iron oxide nanoparticles.

In any case, a number of mechanisms, including: (i) an increase or decrease in crystallinity, (ii) changes in the height of the barrier due to the changes in crystallite dimension, (iii) effects of quantum size, (iv) the density of impurities, and (v) compressive or tensile strains, can contribute to the observed energy gap shifts [22].

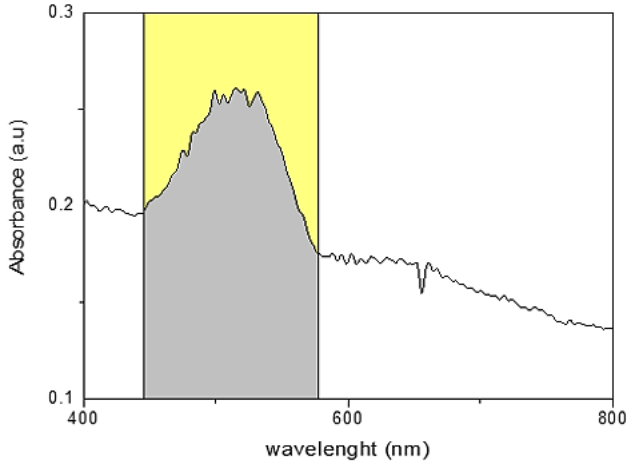

Figure 7: Absorption spectrum of the prepared iron oxide nanoparticles

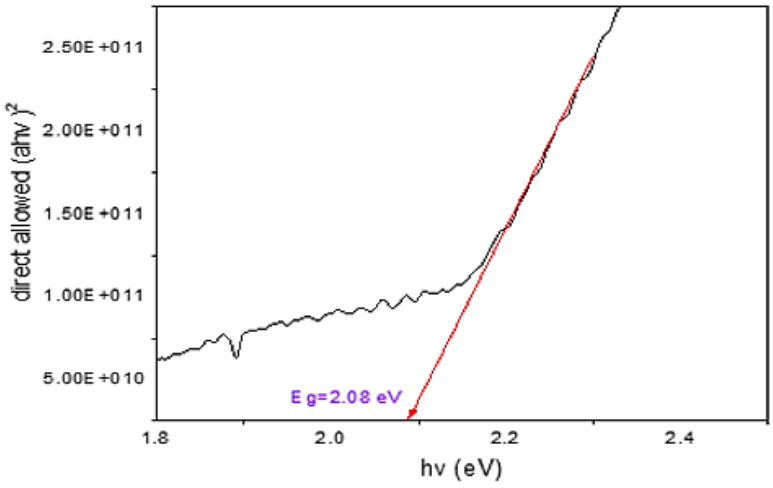

Figure 8: The optical band gap of iron oxide nanoparticles prepared by hydrothermal method

Conclusion

Iron oxide nanoparticles have been successfully prepared through hydrothermal method by using new design homemade autoclave reactor. Surface morphology, structural morphology, and optical studies were studied for preparation of iron oxide nanoparticles. The XRD pattern showed a small particle size for preparing iron oxide with maghemite phase. The structural morphology confirmed the purity of prepared iron oxide

nanoparticles without any impurities, the optical properties indicated that the prepared iron oxide have an optical energy gap about 2.1 eV. Finally, all these results indicate that this homemade autoclave reactor is an excellent design used to synthesize iron oxide nanoparticles with a high purity and small nano size to be used in many applications such as magnetic ink, magnetic storage tape and devices, medicine and medical diagnosis, MRI as a contrast agent, gene and drug delivery, cancer hyperthermia, and wastewater treatment.

Acknowledgments

I am very grateful to Eng. Laila Sarhan from Egypt, and Dr. Raed Muslim from Misan university for their support and guidance in completing this project.

Funding

This research did not receive any specific grant from funding agencies in the public, commercial, or not-for-profit sectors.

Authors' contributions

All authors contributed to data analysis, drafting, and revising of the paper and agreed to be responsible for all the aspects of this work.

Conflict of Interest

There are no conflicts of interest in this study.

References

[1]. Nie S., Xing Y., Kim G.J., Simons J.W., Nanotechnology applications in cancer, *Annual Review of Biomedical Engineering*, 2007, **9**:257 [Crossref], [Google Scholar], [Publisher]

[2]. Miri A., Najafzadeh H., Darroudi M., Miri M.J., Kouhbanani M.A.J., Sarani M., Iron oxide nanoparticles: biosynthesis, magnetic behavior, cytotoxic effect, *ChemistryOpen*, 2021, **10**:327 [Crossref], [Google Scholar], [Publisher]

[3]. Lefebure S., Dubois E., Cabuil V., Neveu S., Massart R., Monodisperse magnetic nanoparticles: preparation and dispersion in water and oils, *Journal of Materials research*, 1998, **13**:2975 [Crossref], [Google Scholar], [Publisher]

[4]. Zhang Z.J., Chen X.Y., Wang B.N., Shi C.W., Hydrothermal synthesis and self-assembly of magnetite (Fe_3O_4) nanoparticles with the magnetic and electrochemical properties. *Journal of crystal growth*, 2008, **310**:5453 [Crossref], [Google Scholar], [Publisher]

[5]. Wu M., Long J., Huang A., Luo Y., Feng S., Xu R., Microemulsion-mediated hydrothermal synthesis and characterization of nanosize rutile and anatase particles, *Frontiers of Chemical Science and Engineering*, 1999, **15**:8822 [Crossref], [Google Scholar], [Publisher]

[6]. Park J., An K., Hwang Y., Park J.G., Noh H.J., Kim J.Y., Park J., Hwang N., Hyeon T., Ultra-large-scale syntheses of monodisperse nanocrystals, *Nature materials*, 2004, **3**:891 [Crossref], [Google Scholar], [Publisher]

[7]. Zhou S.M., Zhao S.Y., He L.F., Guo Y.Q., Shi L., Facile synthesis of Ca-doped manganite nanoparticles by a nonaqueous sol-gel method and their magnetic properties, *Matter, Materials Chemistry and Physics*, 2010, **120**:75 [Crossref], [Google Scholar], [Publisher]

[8]. Cho S.G., Jeon K.W., Kim J., Kim K.H., Kim J., Synthesis and Ferromagnetic Properties of Magnetic Ink for Direct Printing, in *IEEE Transactions on Magnetics, Institute of Electrical and Electronics Engineers*, 2011, **47**:3157 [Crossref], [Google Scholar], [Publisher]

[9]. Jang, J.H., Lim H.B., Characterization and analytical application of surface modified magnetic nanoparticles, *Microchemical Journal*, 2010, **94**:148 [Crossref], [Google Scholar], [Publisher]

[10]. Suna C., Leeb J.S.H., Zhang M., Magnetic nanoparticles in MR imaging and drug delivery, *Advanced Drug Delivery Reviews*, 2008, **60**:1252 [Crossref], [Google Scholar], [Publisher]

[11]. Shi D., Bedford N.M., Cho H., Engineered Multifunctional Nanocarriers for Cancer Diagnosis and Therapeutics., *National Center for Biotechnology Information*, 2011, **7**:2549 [Crossref], [Google Scholar], [Publisher]

[12]. Prabowo B., Khairunnisa T., Nandiyanto A.B.D., Economic Perspective in the Production of Magnetite (Fe_3O_4) Nanoparticles by Co-Precipitation Method, *World Chemical Engineering*

Journal, 2018, **2**:1 [Crossref], [Google Scholar], [Publisher]

[13]. Praserthdam P ., Mekasuwandumrong O., Phungphadung J., Kanyanucharat A., Tanakulrungsank W., New correlation for the effects of the crystallite size and calcination temperature on the single iron oxide nan crystallites, *Crystal Growth and Design*, 2003, **3**:215 [Crossref], [Google Scholar], [Publisher]

[14]. Byrappa K., Adschiri T., Hydrothermal technology for nanotechnology, *Progress in crystal growth and characterization of materials*, 2007, **53**:117 [Crossref], [Google Scholar], [Publisher]

[15]. Zanon Costa C., Falabella Sousa-Aguiar E., Peixoto Gimenes Couto M.A., Souza de Carvalho Filho J.F., Hydrothermal treatment of vegetable oils and fats aiming at yielding hydrocarbons: a review, *Catalysts*, 2020, **10**:843 [Crossref], [Google Scholar], [Publisher]

[16]. Ahmad M.A., Nasiri N.M, Synthesis of maghemite (γ-Fe2O3) nanoparticles by thermal-decomposition of magnetite (Fe_3O_4) nanoparticles*, Materials Science-Poland*, 2013, **31**:264 [Crossref], [Google Scholar], [Publisher]

[17]. Tartaj P., del Puerto Morales M., Veintemillas-Verdaguer S., González-Carreño T., Serna C.J., The preparation of magnetic nanoparticles for applications in biomedicine, *Journal of physics D: Applied physics*, 2003, **36**:182 [Crossref], [Google Scholar], [Publisher]

[18]. Hwang S.W., Umar A., Dar G.N., Kim S.H., Badran R.I., Synthesis and characterization of iron oxide nanoparticles for phenyl hydrazine sensor applications, *Sensor Letters*, 2014, **12**:97 [Crossref], [Google Scholar], [Publisher]

[19]. Abderrahim B., Abderrahman E., Mohamed A., Fatima T., Abdesselam T., Krim O., Kinetic thermal degradation of cellulose, polybutylene succinate and a green composite: comparative study, *World Journal of Environmental Engineering,* 2015, **3**:95 [Crossref], [Google Scholar], [Publisher]

[20]. Eid M.M., Spectroscopic Characterization of Iron Oxide Nanoparticles Functionalized with Chitosan Biosynthesis by a Clean one Pot Method, *Middle East Journal of Applied Sciences*, 2015, **5**:18 [Google Scholar], [Publisher]

[21]. Jozanikohan G., Abarghooei M.N., The Fourier transform infrared spectroscopy (FTIR) analysis for the clay mineralogy studies in a clastic reservoir, *Journal of Petroleum Exploration and Production Technology*, 2022, **12**:2093 [Crossref], [Google Scholar], [Publisher]

[22]. Mariappan R., Ponnuswamy V., Suresh P., Ashok N., Jayamurugan P., Bose A.C., Influence of film thickness on the properties of sprayed ZnO thin films for gas sensor applications, *Superlattices Microstructure*, 2014, **71**:238 [Crossref], [Google Scholar], [Publisher]

HOW TO CITE THIS ARTICLE

Ahmed B. Taha, Mohammed Sh. Essa, Bahaa T. Chiad. Spectroscopic Study of Iron Oxide Nanoparticles Synthesized Via Hydrothermal Method. *Chem. Methodol.*, 2022, 6(12) 977-984

https://doi.org/10.22034/CHEMM.2022.355199.1590

URL: http://www.chemmethod.com/article_156783.html